The REVEILLE Clock Genes Inhibit Growth of Juvenile and Adult Plants by Control of Cell Size[1][OPEN]

Jennifer A. Gray, Akiva Shalit-Kaneh, Dalena Nhu Chu, Polly Yingshan Hsu[2], and Stacey L. Harmer*

Department of Plant Biology, College of Biological Sciences, University of California, Davis, California 95616

ORCID IDs: 0000-0002-7078-0132 (A.S.-K.); 0000-0001-7071-5798 (P.Y.H.); 0000-0001-6813-6682 (S.L.H.).

The circadian clock is a complex regulatory network that enhances plant growth and fitness in a constantly changing environment. In Arabidopsis (*Arabidopsis thaliana*), the clock is composed of numerous regulatory feedback loops in which *REVEILLE8* (*RVE8*) and its homologs *RVE4* and *RVE6* act in a partially redundant manner to promote clock pace. Here, we report that the remaining members of the *RVE8* clade, *RVE3* and *RVE5*, play only minor roles in the regulation of clock function. However, we find that RVE8 clade proteins have unexpected functions in the modulation of light input to the clock and the control of plant growth at multiple stages of development. In seedlings, these proteins repress hypocotyl elongation in a daylength- and sucrose-dependent manner. Strikingly, adult *rve4 6 8* and *rve3 4 5 6 8* mutants are much larger than wild-type plants, with both increased leaf area and biomass. This size phenotype is associated with a faster growth rate and larger cell size and is not simply due to a delay in the transition to flowering. Gene expression and epistasis analysis reveal that the growth phenotypes of *rve* mutants are due to the misregulation of *PHYTOCHROME INTERACTING FACTOR4* (*PIF4*) and *PIF5* expression. Our results show that even small changes in *PIF* gene expression caused by the perturbation of clock gene function can have large effects on the growth of adult plants.

Circadian rhythms are endogenous, biological rhythms that oscillate with an ~24-h period. These rhythms are observed in many organisms throughout nature (Dunlap, 1999; Harmer et al., 2001; Harmer, 2009), and are particularly vital for plants due to their sessile nature. Numerous studies in plants have indicated that an impaired circadian oscillator can contribute to diminished growth, impaired defense against herbivores and pathogens, and even reduced fitness (Green et al., 2002; Dodd et al., 2005; Yerushalmi et al., 2011; Goodspeed et al., 2012; Ruts et al., 2012).

The molecular network of the Arabidopsis (*Arabidopsis thaliana*) circadian clock is composed primarily of transcription factors that regulate each other's as well as their own expression (Hsu and Harmer, 2014; McClung, 2014). Two homologous single MYB-like domain transcription factors, *CIRCADIAN CLOCK ASSOCIATED1* (*CCA1*) and *LATE ELONGATED HYPOCOTYL* (*LHY*; Schaffer et al., 1998; Wang and Tobin, 1998), have a circadian pattern of transcript peaking at dawn, and loss-of-function mutants have a short free-running period in continuous light (Green and Tobin, 1999; Alabadí et al., 2002; Mizoguchi et al., 2002). CCA1 and LHY comprise a negative feedback loop with *TIMING OF CAB EXPRESSION1* (*TOC1*) in which they bind to the evening element promoter motif of this and other evening-phased clock genes to repress expression during the day (Alabadí et al., 2002; Harmer and Kay, 2005; Nagel et al., 2015). TOC1 in turn regulates *CCA1* and *LHY* by repressing their expression in a time-of-day-dependent manner (Gendron et al., 2012; Huang et al., 2012; Pokhilko et al., 2012).

More recent work has characterized the role of the transcription factor *REVEILLE8* (*RVE8*), a homolog of *CCA1* and *LHY*, in the circadian network (Farinas and Mas, 2011; Rawat et al., 2011). These transcription factors are deemed members of the core oscillator, as mutation of any one of these genes results in a free-running clock period that is either longer or shorter than in the wild type. Specifically, while *cca1* and *lhy* mutants have a short period, the *rve8* loss-of-function mutant has a long free-running period (Farinas and Mas, 2011; Rawat et al., 2011). Although RVE8 binds to similar evening-phased gene targets as CCA1 and LHY, this transcription factor activates instead of represses target gene expression (Farinas and Mas, 2011; Rawat et al., 2011; Hsu et al., 2013), explaining the opposite period phenotypes of these mutants. RVE8 forms an additional feedback loop in the clock, in which it positively regulates the evening-expressed transcription factor *PSEUDO RESPONSE REGULATOR5* (*PRR5*), whose protein in turn represses the expression of *RVE8* (Rawat et al., 2011).

[1] This work was supported by the National Institutes of Health (grant no. GM069418 to S.L.H.).

[2] Present address: Department of Biology, Duke University, Durham, NC 27708.

* Address correspondence to slharmer@ucdavis.edu.

The author responsible for distribution of materials integral to the findings presented in this article in accordance with the policy described in the Instructions for Authors (www.plantphysiol.org) is: Stacey L. Harmer (slharmer@ucdavis.edu).

J.A.G., A.S.-K., P.Y.H., and S.L.H. designed the research; J.A.G., A.S.-K., D.N.C., and P.Y.H. performed the research; J.A.G., A.S.-K., P.Y.H., and S.L.H. analyzed data; J.A.G. and S.L.H. wrote the article.

[OPEN] Articles can be viewed without a subscription.

www.plantphysiol.org/cgi/doi/10.1104/pp.17.00109

RVE8 is one of 11 homologous MYB-like transcription factors in Arabidopsis (Rawat et al., 2009). RVE8 acts in a partially redundant manner with *RVE4* and *RVE6*, two closely related genes, to promote clock pace (Hsu et al., 2013). Two remaining members of the *RVE8* clade, RVE3 and RVE5, were found to associate with the evening element promoter motif both in vitro and in vivo (Gong et al., 2008; Rawat et al., 2011). However, their role in the clock has not been characterized previously.

Additional key clock proteins include the transcription factors EARLY FLOWERING3 (ELF3), ELF4, and LUX ARRYTHMO (LUX), which together constitute the tripartite evening complex (EC; Nusinow et al., 2011). Each component of the EC is necessary for its function, as the *lux*, *elf3*, and *elf4* single mutants are all arrhythmic in continuous light (Hicks et al., 2001; Doyle et al., 2002; Hazen et al., 2005). The EC forms in the early evening and acts to regulate numerous downstream genes as well as the expression of other clock components (Dixon et al., 2011; Helfer et al., 2011; Nusinow et al., 2011; Mizuno et al., 2014).

Approximately one-third of the Arabidopsis transcriptome is under circadian control (Covington et al., 2008), and consistent with this, many aspects of plant growth and development are influenced by the circadian clock (Farré, 2012; Song et al., 2013). Hypocotyl and root elongation and leaf growth undergo daily rhythms, and the phases of peak growth rates are shifted but not abolished in constant environment conditions (Nozue et al., 2007; Poiré et al., 2010; Iijima and Matsushita, 2011; Yazdanbakhsh et al., 2011).

The clock is vital for growth rhythms in multiple organs, as the leaves and roots of the arrhythmic circadian mutants *cca1-ox* and *prr9 7 5* exhibit perturbed growth (Ruts et al., 2012). The clock also modulates the timing of the transition from vegetative to reproductive growth by controlling the rhythmic oscillations of key transcriptional regulators that promote flowering (Song et al., 2013). Flowering time also is regulated by light signaling pathways, which modulate the stability of clock-regulated proteins to control their activity in a daylength-dependent manner (Song et al., 2013).

Many other developmental pathways are regulated not only by the clock but also by environmental stimuli. Hypocotyl elongation in Arabidopsis is influenced by changes in light and temperature as well as by the clock (Nozue et al., 2007; Nomoto et al., 2012). Two key regulators of hypocotyl elongation are the basic helix-loop-helix transcription factors *PHYTOCHROME INTERACTING FACTOR4* (*PIF4*) and *PIF5* (Leivar et al., 2008, 2012; Lorrain et al., 2008; Hornitschek et al., 2012). The differential patterns of hypocotyl growth in constant light and in light/dark cycles are due to the EC-mediated circadian regulation of *PIF4* and *PIF5* expression (Nusinow et al., 2011) combined with the posttranslational regulation of PIF protein stability by red light-activated phytochrome (Nozue et al., 2007; Lorrain et al., 2008). In addition, PIF4 and PIF5 influence the rhythmic growth of leaves (Dornbusch et al., 2014). PIF proteins also have been shown to act in many other response pathways, such as auxin (Franklin et al., 2011; Kunihiro et al., 2011; Nozue et al., 2011; Hornitschek et al., 2012; Sun et al., 2012), gibberellin (de Lucas et al., 2008), high temperature (Koini et al., 2009; Stavang et al., 2009), and sucrose (Liu et al., 2011; Stewart et al., 2011).

Although the roles of the circadian clock and PIFs in the regulation of hypocotyl elongation in Arabidopsis have been examined thoroughly, clock modulation of growth in adult plants is much less understood. Here, we demonstrate that the loss of RVE function alters *PIF* gene expression. Surprisingly, this perturbation causes greatly enhanced growth at both juvenile and mature stages of development, resulting in increased cell size and greater aerial biomass in *rve* mutants than in wild-type controls. These data provide a rare example in which the alteration of circadian clock function promotes instead of inhibits plant growth, potentially opening up novel agricultural applications.

RESULTS

The *RVEs* Act in a Partially Redundant Manner to Promote the Pace of the Clock

Previous work has demonstrated that multiple members of the *RVE* family of transcription factors help control the pace of the circadian clock. Whereas mutations in the MYB-like transcription factors *CCA1* and *LHY* shorten clock pace (Green and Tobin, 1999; Alabadí et al., 2002; Mizoguchi et al., 2002), mutations in their homolog *RVE8* and two closely related genes, *RVE4* and *RVE6*, lengthen the circadian period (Farinas and Mas, 2011; Rawat et al., 2011; Hsu et al., 2013).

RVE3 and *RVE5* are the remaining members of the RVE8 clade. To investigate their role in clock function, we first identified plants with T-DNA insertions within these two genes. Neither *RVE3* nor *RVE5* was detectably expressed in the *rve3-1* (SALK_001480C) or *rve5-1* (SAIL_769_A09) mutant, respectively (Supplemental Fig. S1). As neither single mutant has a detectable circadian clock phenotype (data not shown), we examined the free-running circadian period in *rve3-1 rve5-1* (*rve3 5*) mutants harboring a clock-regulated luciferase reporter construct (*CCR2*::*LUC*). In contrast to the long-period phenotype of the *rve4-1 rve6-1 rve8-1* (*rve4 6 8*) triple mutant (Hsu et al., 2013), the *rve3 5* double mutant displays a slightly shorter free-running period than wild-type Columbia (Col = 23.95 ± 0.09 h, *rve4 6 8* = 27.83 ± 0.7 h, and *rve3 5* = 23.63 ± 0.04 h; Fig. 1). Although the period of the *rve3 5* double mutant is statistically significantly different from that of the wild type, the subtle difference in clock pace compared with the wild type suggests that *RVE3* and *RVE5* do not play a major role in clock function.

We next examined whether *RVE3* and *RVE5* play a partially redundant role in the clock with their homologs *RVE4*, *RVE6*, and *RVE8*. In contrast to the slightly

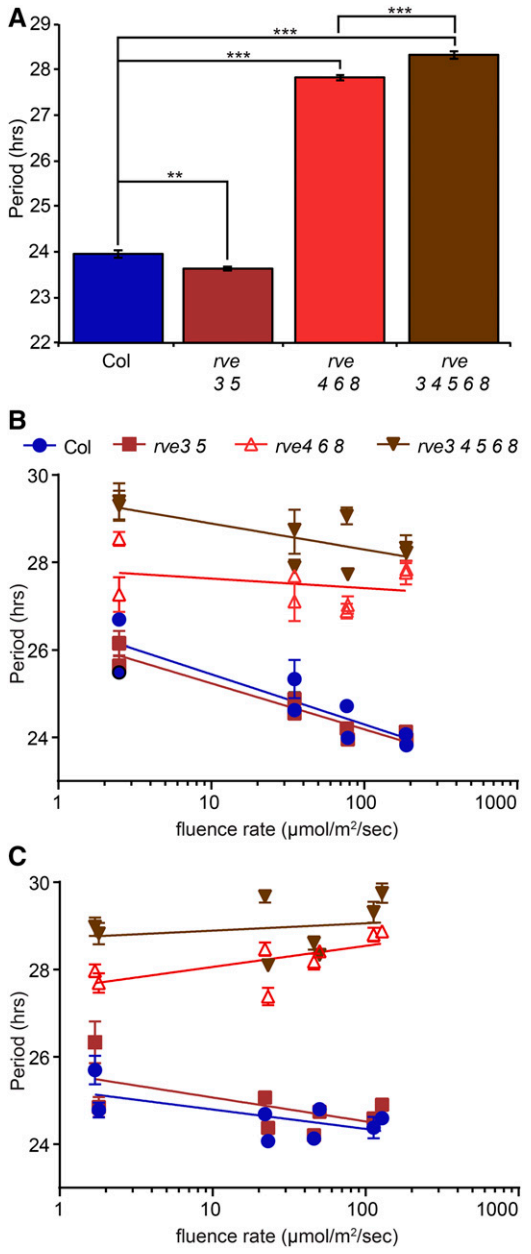

Figure 1. Free-running circadian period is lengthened in *rve* triple and quintuple mutants. Plants were entrained for 6 d in 12-h-light/12-h-dark cycles at 22°C before release to constant light (LL) at the indicated fluence rates at 22°C. A, *CCR2*::*LUC* expression was assayed in constant red plus blue light (86 μmol m^{-2} s^{-1} total fluence, equal contributions red and blue light; n = 35–45). B, Fluence rate response curves for *CCR2*::*LUC* period in constant red light (n = 20–30). C, Fluence rate response curves for *CCR2*::*LUC* period in constant blue light (n = 20–30). Error bars represent SE. **, $P < 0.01$ and ***, $P < 0.001$, Student's t test. Data shown are illustrative of at least two independent experiments.

shorter period seen in *rve3 5* double mutants compared with the wild type, plants mutant for all five *RVE8*-related transcription factors (*rve3 4 5 6 8*) have a slightly longer free-running period than the *rve4 6 8* triple mutant (*rve4 6 8* = 27.83 ± 0.7 h and *rve3 4 5 6 8* = 28.33 ± 0.09 h). The difference in period between the *rve* triple and quintuple mutants is small, although statistically significant (Fig. 1). This result further indicates a modest role for *RVE3* and *RVE5* in the control of clock pace.

We next examined whether the sensitivity of the circadian clock to light is altered in *rve* mutants. For this, we examined the effects of different fluence rates of monochromatic red and blue light on free-running circadian period. Mutations in light signaling components have been shown previously to alter the relationship between free-running period and fluence rate (Somers et al., 1998; Devlin and Kay, 2000). We found that the shortening of the period in response to high fluence rates of monochromatic red light seen in Col and *rve3 5* is less pronounced in *rve4 6 8* and *rve3 4 5 6 8* (Fig. 1), suggesting reduced sensitivity of the clock to red light in these mutants. Surprisingly, *rve* triple and quintuple mutants in monochromatic blue light have longer free-running periods at higher than at lower fluence rates, the opposite of the trend seen in the wild type (Fig. 1). Thus, clock responsiveness to blue light is fundamentally different in the *rve* mutants than in control plants. Together, these data indicate that the RVEs affect both red and blue light signaling to the circadian clock, but in a distinct manner.

Flowering Time Is Modestly Delayed in the *rve* Mutants

The circadian clock plays an important role in the daylength-dependent control of the transition from vegetative to reproductive growth (Song et al., 2013). To determine whether the *RVE*s play an important role in the regulation of flowering time, we examined both leaf number and days to bolting in Col, *rve4 6 8*, and *rve3 4 5 6 8* mutants grown in long-day (LD; 16-h-light/8-h-dark) conditions. In our growth conditions, wild-type plants bolt after ~24 d, while flowering time in the *rve4 6 8* triple mutant is delayed by an average of 3 d. The *rve3 4 5 6 8* quintuple mutant flowers significantly later than the triple mutant, at ~29 d (Fig. 2). These slight delays in the timing of the transition to flowering are mirrored by changes in leaf number at bolting, with the *rve4 6 8* mutant generating an average of two more and *rve3 4 5 6 8* an average of three more rosette leaves than the wild type (Fig. 2). Thus, the *RVE8* clade genes play a minor role in the control of flowering time.

Daylength Dependence of *RVE* Mutant Hypocotyl Phenotypes

The circadian clock drives the rhythmic oscillations of hypocotyl elongation in Arabidopsis, and mutations in many clock genes result in seedlings with perturbed hypocotyl growth patterns (Farré, 2012). Since *RVE8* clade genes affect clock pace, we investigated the hypocotyl phenotypes of the *rve* triple and quintuple

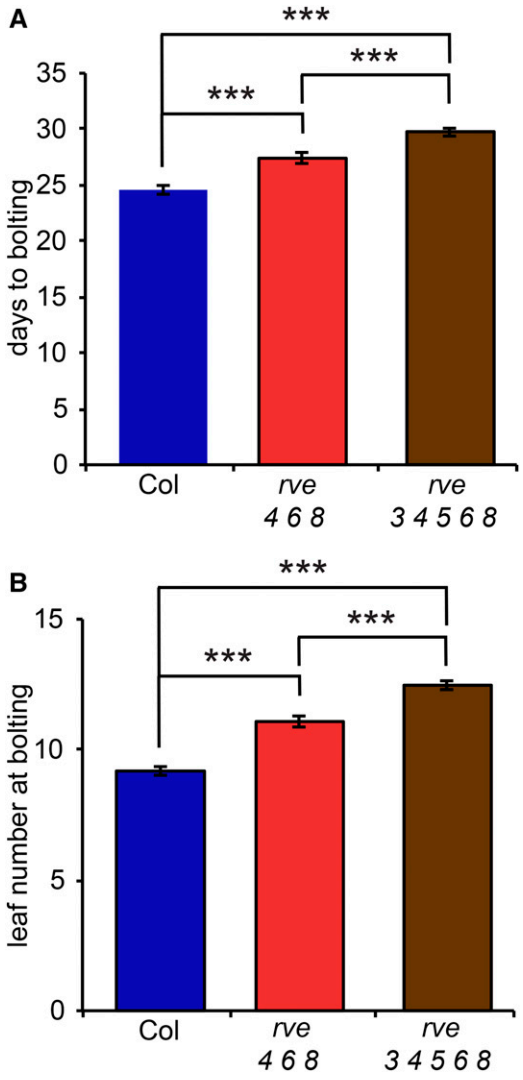

Figure 2. Flowering time is delayed modestly in *rve* mutants. Plants were grown in LD cycles. Bolting date was defined as the day at which the inflorescence reached 1 cm. A, Days to bolting (n = 25–36). B, Rosette leaf number at bolting (n = 25–36). Error bars represent SE. ***, $P < 0.001$, Student's t test. Data shown are illustrative of at least two independent experiments.

mutants at various intensities of white light and under different daylengths.

When grown in short-day (SD) conditions (8 h of light/16 h of dark), both wild-type and *rve* mutant plants show inhibition of hypocotyl elongation in response to increasing fluence rates of light (Fig. 3). However, the hypocotyl lengths of the *rve* triple and quintuple mutants are significantly longer than those of the wild type at all fluence rates tested, with the maximal difference between the mutants and the wild type occurring at the highest fluence rate tested (100 μmol m^{-2} s^{-1} white light; Fig. 3). In LD conditions, hypocotyl lengths of the *rve* triple and quintuple mutants are significantly different from those of the wild type at mid to high light intensities (7.5–50 μmol m^{-2} s^{-1}) but not at the lowest (0.6 μmol m^{-2} s^{-1}) or highest (100 μmol m^{-2} s^{-1}) fluence rates tested (Fig. 3). Similar to LD conditions, hypocotyls of the *rve4 6 8* and *rve3 4 5 6 8* mutants are longer than wild-type hypocotyls at mid-range intensities (7.5–25 μmol m^{-2} s^{-1}) of LL but are no different from the control at very low (0.6 μmol m^{-2} s^{-1}) or high (50–80 μmol m^{-2} s^{-1}) fluence rates (Fig. 3). The hypocotyl lengths of *rve4 6 8* and *rve3 4 5 6 8* are not significantly different from each other under any of the conditions tested. Taken together, these data indicate that *RVE4*, *RVE6*, and *RVE8* contribute to the regulation of hypocotyl length in a fluence rate- and daylength-dependent manner and that *RVE3* and *RVE5*

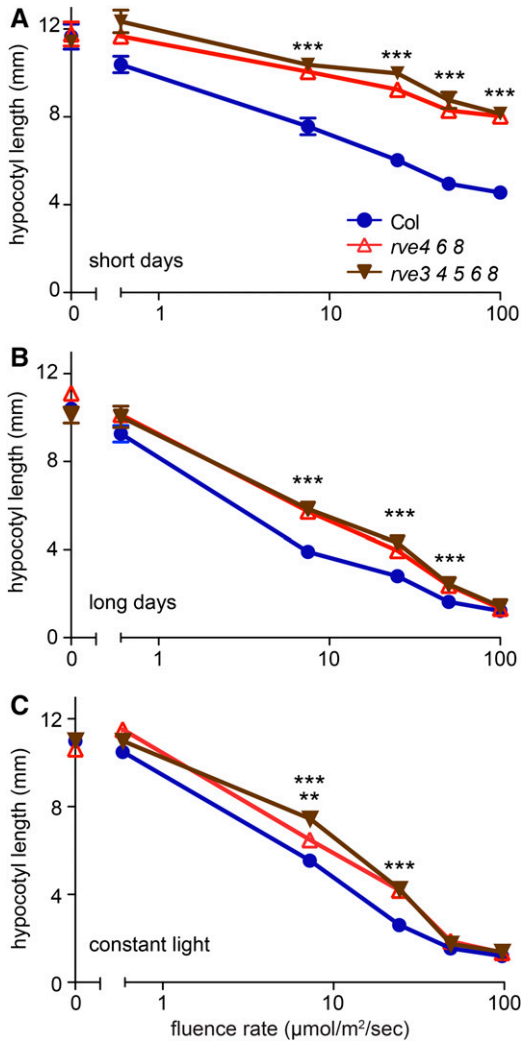

Figure 3. Hypocotyl lengths of Col and *rve* mutant plants grown in different photoperiods. Seedlings were grown at 22°C in white light at the indicated fluence rates for 7 d. A, Hypocotyl lengths of Col and *rve* mutants in SD conditions (n = 15–40). B, Hypocotyl lengths in LD conditions (n = 23–35). C, Hypocotyl lengths in LL conditions (n = 20–40). Error bars represent SE. **, $P < 0.01$ and ***, $P < 0.001$, Student's t test. Data shown are illustrative of at least two independent experiments.

do not contribute significantly to this phenotype in the conditions tested.

The *RVEs* Repress Growth in Adult Plants

Since we found that the *RVEs* influence growth at the seedling stage, we investigated if this also is true at later stages of development by measuring the rosette diameter of 6-week-old plants grown in LD conditions. We found that both *rve4 6 8* and *rve3 4 5 6 8* are ~1.5-fold larger in diameter than the wild type (Fig. 4). To determine if this rosette size difference is associated with increased biomass, we measured the dry weight of aerial tissues of plants harvested at 6 weeks of age. Strikingly, the *rve* triple and quintuple mutants exhibit an ~30% increase in aerial dry weight compared with the wild type (Fig. 4). There is no significant difference in aerial biomass between the *rve* triple and quintuple mutants, indicating that *RVE3* and *RVE5* do not contribute significantly to growth regulation in LD conditions (Fig. 4).

To determine whether the extra rosette leaves made by the *rve* mutants before the transition to flowering (Fig. 2) could account for the increased growth of these mutants, we assessed rosette diameter by measuring the distance between leaves 8 and 9, which were produced by all genotypes. As measured this way, the rosette diameter of *rve4 6 8* and *rve3 4 5 6 8* mutants is ~25% larger than that of the wild-type controls (Fig. 4), demonstrating a growth phenotype in these plants independent of the flowering time phenotype.

We next measured blade area, blade length, and petiole length of leaves 8 and 9 in the *rve* mutants to determine what aspects of leaf development are affected. The blade area of both leaves 8 and 9 is increased ~20% to 30% in the triple and quintuple *rve* mutants compared with the wild type (Fig. 4). The average blade length of leaf 8 also is increased by about 20%, being ~7 mm longer ($P = 6.4 \times 10^{-4}$) in the *rve* triple mutant and ~9 mm longer ($P = 4.8 \times 10^{-5}$) in the *rve* quintuple mutant relative to the wild type. Likewise, the blade length of leaf 9 is increased by ~8 mm ($P = 1.6 \times 10^{-4}$) and ~10 mm ($P = 5.6 \times 10^{-6}$) in the *rve* triple and quintuple mutants, respectively, compared with the wild type (Fig. 4). The difference in average petiole length is similar between the two mutants and the wild type, with an increase in petiole length of ~7 to 8 mm ($P < 5 \times 10^{-4}$) in *rve4 6 8* and ~9 to 10 mm ($P < 5 \times 10^{-3}$) in *rve3 4 5 6 8* relative to controls (Fig. 4). Thus, many aspects of leaf growth are enhanced in *rve* mutants.

We also measured these growth parameters at 3 weeks of age, before the transition to bolting in both wild-type and *rve* mutant plants. Similar to later stages of growth, *rve* triple and quintuple mutants both display significant increases in blade area, blade length, and petiole length compared with the wild type when grown in LD conditions (Supplemental Fig. S2). In contrast, blade area and length are not significantly

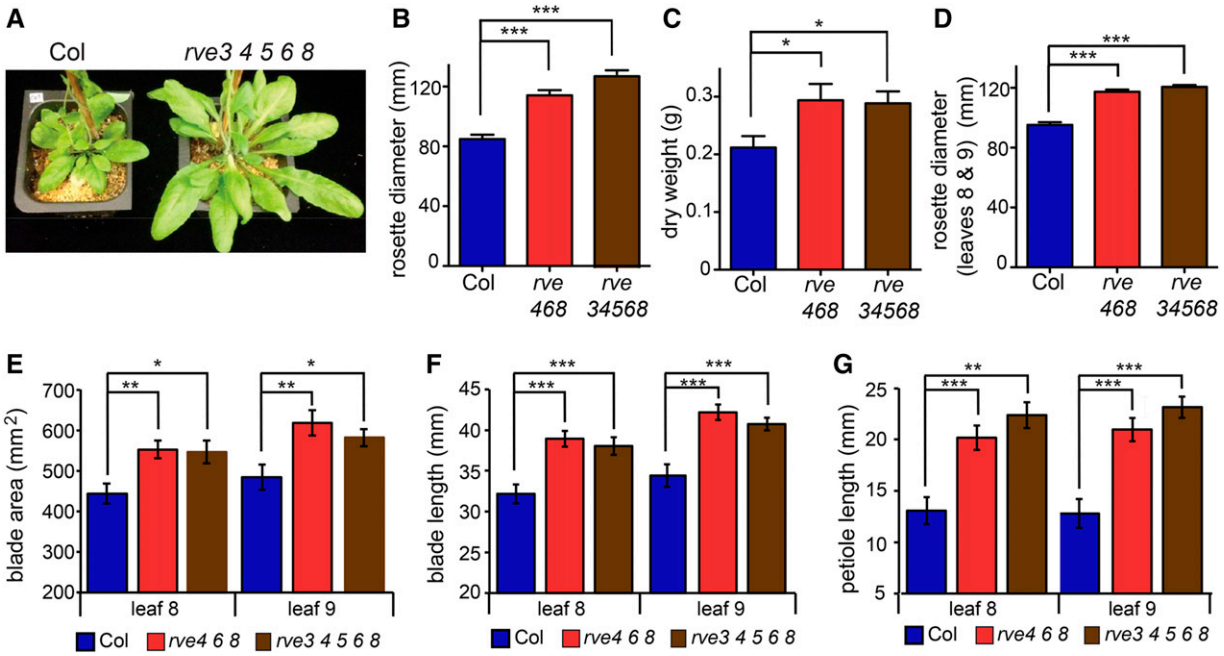

Figure 4. Aerial growth phenotypes of 6-week-old Col and *rve* mutant plants. Plants were grown in LD cycles (55 μmol m^{-2} s^{-1} white light) for 6 weeks. A, Col and *rve3 4 5 6 8* plants. B, Rosette diameter measured at the greatest distance between leaves of Col, *rve4 6 8*, and *rve3 4 5 6 8* plants ($n = 28$–33). C, Biomass measured as total aerial dry weight ($n = 16$–23). D, Rosette diameter measured as the distance between leaves 8 and 9 ($n = 28$–33). E, Blade areas of leaves 8 and 9 ($n = 12$). F, Blade lengths of leaves 8 and 9 ($n = 12$). G, Petiole lengths of leaves 8 and 9 ($n = 12$). Error bars represent SE. *, $P < 0.05$; **, $P < 0.01$; and ***, $P < 0.001$, Student's *t* test. Data shown are illustrative of at least two independent experiments.

different between the *rve* mutants and the wild type grown in SD conditions, although petiole length in the mutants is greater than in the controls in both SD and LD conditions. Most leaf parameters are not significantly different between *rve4 6 8* and *rve3 4 5 6 8*. However, the *rve3 4 5 6 8* mutant has a significantly longer petiole than *rve4 6 8* in SD conditions but not in LD conditions (Supplemental Fig. S2). This suggests that the roles of *RVE3* and *RVE5* are influenced by environmental factors. Together, our data show that members of the *RVE8* clade are inhibitors of plant growth at both the seedling and adult stages of development and across different environmental conditions.

Growth Rate Is Accelerated in *rve* Mutants

To better understand why *rve* mutants are larger than wild-type plants, we investigated if the *rve* leaves expand at a faster rate or grow for a longer period of time than in control plants. To avoid the confounding effects of differences in flowering time, we measured rosette diameter as the distance between leaves 8 and 9, which are produced by all genotypes. Significant differences in rosette diameter are evident for both the *rve* triple and quintuple mutants throughout all stages of growth, long before the transition to flowering (Fig. 5). Both mutant and wild-type plants ceased rosette expansion ~30 d after germination, indicating that the larger size of *rve* mutants is due to a faster growth rate rather than an extended period of leaf growth. These data demonstrate that the larger rosette size in adult *rve* mutants is partly caused by an enhanced growth rate of individual leaves and not just a delay in flowering time.

We examined whether this increased growth rate is due to larger average cell size or more cells per organ in the mutant compared with the control. We found that the average area of mesophyll cells in the leaves of 6-week-old *rve4 6 8* mutants is increased by ~30% compared with the wild type (Col = 7.01×10^3 μm^2 and *rve4 6 8* = 9.27×10^3 μm^2; $P = 5.3 \times 10^{-36}$; Fig. 5). This increase in cell size is similar to the increase in total blade area in the mutant (Fig. 4), suggesting that the larger average cell size is primarily responsible for the increased leaf size in *rve* mutants.

rve Mutants Display an Enhanced Sensitivity to Sucrose

Sugars are well-known regulators of plant growth (Lastdrager et al., 2014). Therefore, we investigated whether *rve* mutants have an altered response to sucrose. We grew *rve4 6 8*, *rve3 4 5 6 8*, and Col seedlings on various concentrations of sucrose in 12-h-light/12-h-dark conditions and measured hypocotyl lengths. The maximal enhancement of hypocotyl elongation for all genotypes occurred at 2% sucrose and diminished at higher concentrations (Fig. 6). We next examined

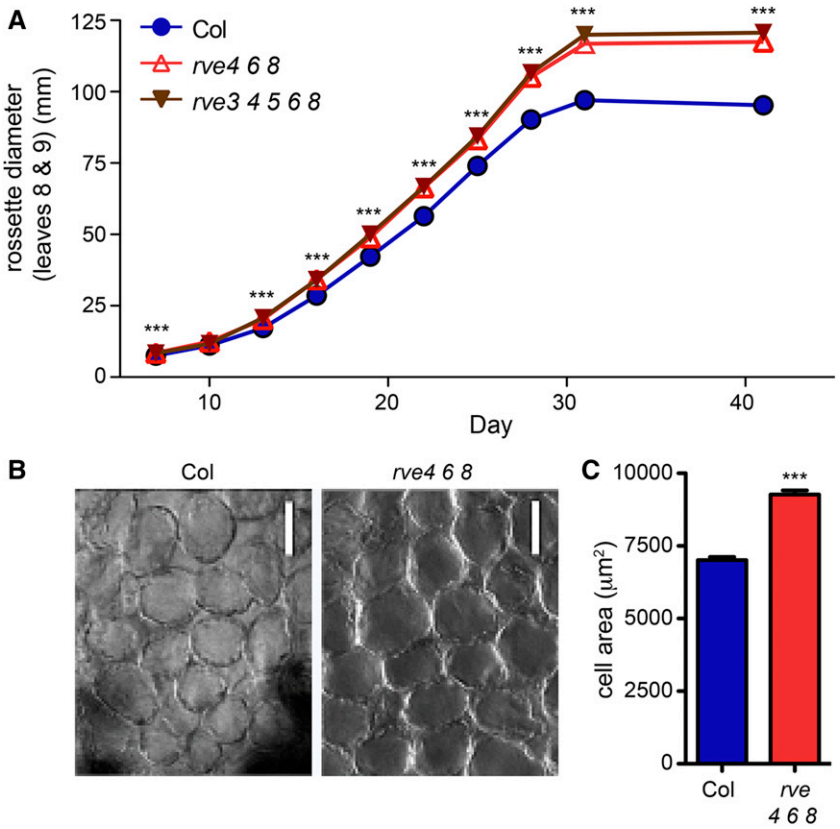

Figure 5. The *RVEs* reduce rosette growth rate and cell size. Col, *rve4 6 8*, and *rve3 4 5 6 8* plants were grown in LD cycles (55 μmol m^{-2} s^{-1} white light). A, Rosette diameter measured as the distance between leaves 8 and 9 (n = 28–33). Asterisks indicate significant differences between the mutants and Col: ***, $P < 0.001$, Student's t test. B, Size of leaf blade mesophyll cells in 6-week-old Col and *rve4 6 8* plants (n = 12 leaves per genotype and n = 20–40 cells per leaf). Images were taken at 20× magnification with a Zeiss Axioscop 2 plus microscope. Bars = 100 μm. C, Quantification of mesophyll cell area. Error bars represent SE. ***, $P < 0.001$, Student's t test. Data shown are illustrative of at least two independent experiments.

responsiveness to sucrose by comparing the degree of sucrose-mediated growth enhancement relative to the no-sucrose controls for each genotype (Fig. 6). Notably, both *rve* triple and quintuple mutants displayed an enhanced response to sucrose compared with Col at concentrations of sucrose between 0.5% and 3% (Fig. 6). The *rve* quintuple mutant demonstrated an even greater response to sucrose than the *rve* triple mutant at 2% and 6% sucrose (Fig. 6), suggesting that *RVE3*, *RVE5*, or both act in a partially redundant manner with *RVE4*, *RVE6*, and *RVE8* to repress sucrose growth responses.

Expression of *PIF* Transcription Factors Is Altered in *rve* Mutants

Previous studies have revealed a role for the clock-regulated transcription factors PIF4 and PIF5 in the promotion of hypocotyl elongation in response to sucrose (Liu et al., 2011; Stewart et al., 2011). Since the *rve* mutants are hyperresponsive to sucrose (Fig. 6), we investigated whether *PIF* expression patterns are altered in *rve* mutants in either constant light and/or light/dark cycles. First, wild-type and mutant seedlings were grown in light/dark cycles and then transferred to constant light and temperature conditions at dawn (Zeitgeber time 0). After 32 h in constant conditions, plants were harvested at 3-h intervals and gene expression was determined using quantitative reverse transcription (qRT)-PCR. As expected given the long-period phenotype of *rve4 6 8* mutants (Fig. 1), the circadian patterns of expression of both *PIF4* and *PIF5* show obvious phase delays (Fig. 7; Supplemental Fig. S3). Notably, the maximal abundance of *PIF4* and *PIF5* is not appreciably different from that of the wild type in these conditions. However, the waveforms of *PIF* gene expression are altered in *rve4 6 8* such that trough levels of *PIF* gene expression are increased during the subjective night (Zeitgeber time 36–48) and the peaks of gene expression are broader (Fig. 7). This suggests that overall *PIF* expression levels may be higher in the mutant than in the wild type. Indeed, quantification of *PIF4* and *PIF5* expression across the entire LL time series, determined by computing the area under the curves using natural cubic spline interpolation, reveals significantly greater expression levels in the *rve* mutant compared with the wild type (Fig. 7). These data suggest that the growth phenotypes of *rve* mutants maintained in constant light (Fig. 3) might be due to increased overall levels of *PIF* gene expression.

We next examined *PIF* expression in seedlings grown in LD and SD cycles (Fig. 7; Supplemental Fig. S3). Similar to the LL data, we saw no difference in peak levels of *PIF4* and *PIF5* expression but did see an increase in trough levels. Quantification of *PIF* gene expression across the entire LD and SD time courses did not reveal significant differences between the *rve* mutant and the wild type (data not shown). However, since PIF4 and PIF5 proteins are destabilized in the light (Nozue et al., 2007; Lorrain et al., 2008), differences in transcript levels at night are likely to be of greatest biological significance. Therefore, we calculated *PIF* mRNA expression levels integrated across only the dark portions of the LD and SD time series. We found significantly higher nighttime levels of *PIF4* and *PIF5* expression in LD conditions in the *rve* mutant compared with the wild type. In SD conditions, the differences in *PIF* expression between the genotypes were smaller, reaching statistical significance for *PIF4* but not *PIF5* (Fig. 7). These data suggest that the enhanced growth phenotypes of *rve* mutants in light/dark cycles (Figs. 3–5) might be due to increased levels of *PIF* expression during the night.

The expression of *PIF4* and *PIF5* is repressed directly by multiple clock components, including the EC (Nusinow et al., 2011), PRR5 (Kunihiro et al., 2011; Nakamichi et al., 2012), and TOC1 (Huang et al., 2012). Since we previously reported that RVE8 directly

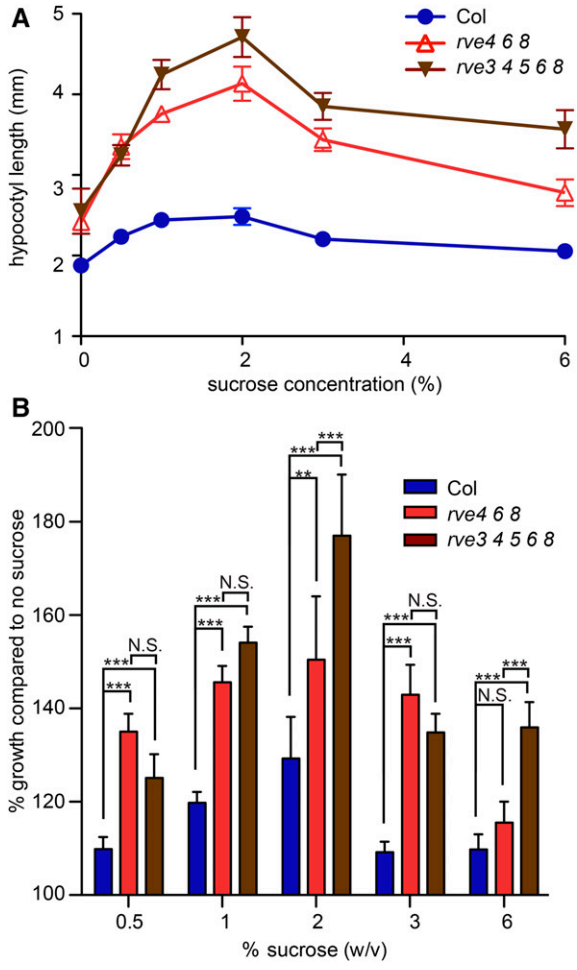

Figure 6. The *RVEs* repress growth responses to sucrose. A, Hypocotyl lengths of 6-d-old seedlings grown in 12-h-light/12-h-dark cycles (55 μmol m^{-2} s^{-1} white light) at 22°C (n = 28–47) with the indicated concentrations of sucrose in the medium. B, As above, but hypocotyl lengths were normalized within each genotype so that the 0% sucrose control = 100%. **, $P < 0.01$ and ***, $P < 0.001$, Student's t test; N.S., not significant.

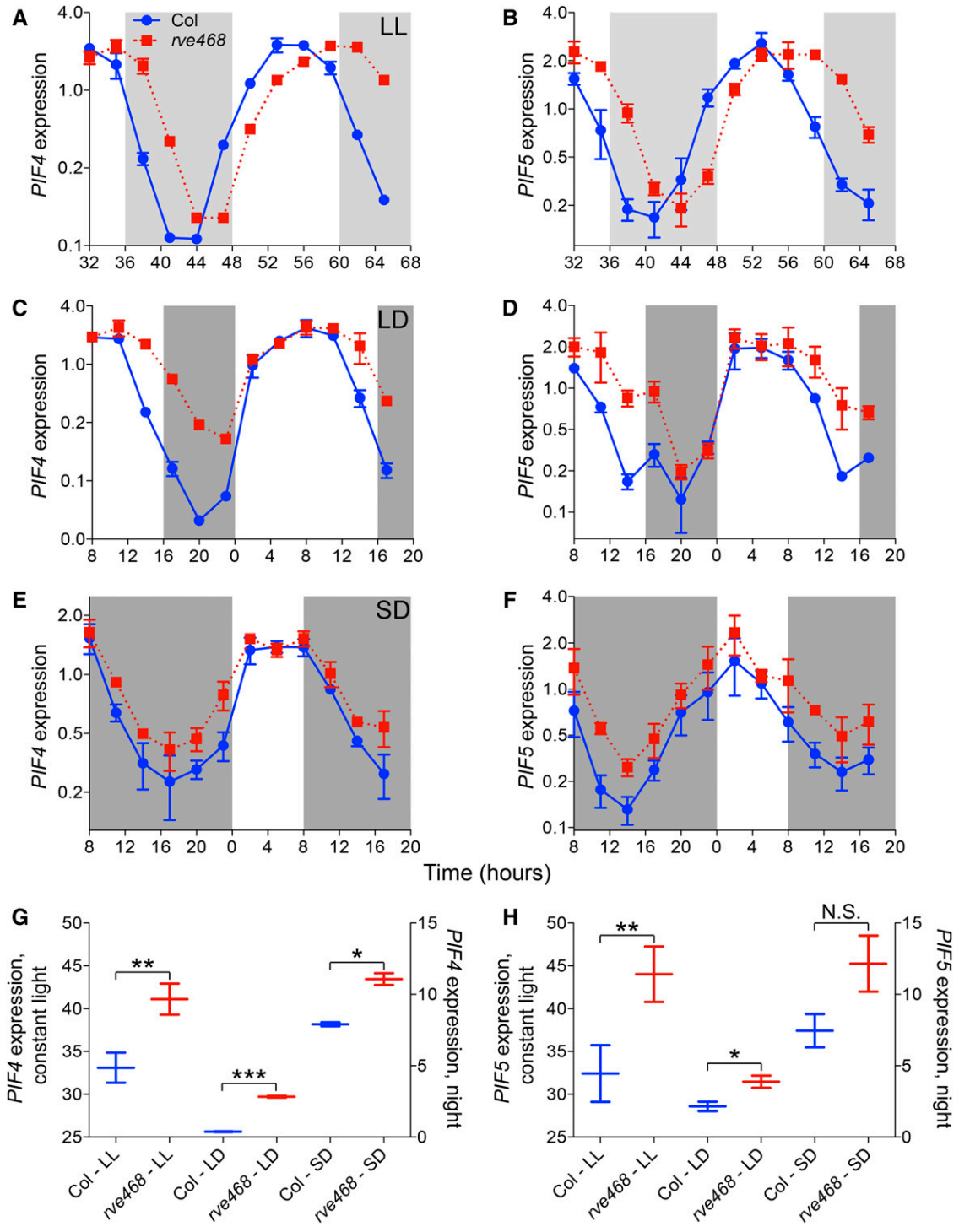

Figure 7. *PIF4* and *PIF5* expression is elevated in *rve4 6 8* mutants. A to F, Time course of *PIF4* and *PIF5* expression. Seedlings were grown in 12-h-light/12-h-dark cycles at 25 μmol m^{-2} s^{-1} white light for 6 d before transfer to LL at the same fluence rate (A and B) or in LD cycles (C and D) or SD cycles (E and F) under 25 μmol m^{-2} s^{-1} white light. *PIF4* (A, C, and E) and *PIF5* (B, D, and F) expression was normalized relative to *PP2a*. Times represent hours since the last transition from dark to light; error bars represent SE of two independent biological replicates. G and H, Expression of *PIF4* (G) or *PIF5* (H) integrated across the entire LL time series (left *y* axes) or during the dark portions of the LD and SD time series (right *y* axes) computed as the area under the curve. Error bars represent the range of values across two independent time-course experiments. ***, $P < 0.001$; **, $P < 0.005$; and *, $P < 0.05$, linear mixed-effect model with genotype as a fixed effect and replicate as a random effect; N.S., not significant.

induces the expression of *PRR5*, *TOC1*, and *LUX*, a member of the EC (Hsu et al., 2013), we examined transcript levels of these genes in *rve4 6 8* mutants and wild-type plants grown in LL, LD, and SD conditions (Supplemental Figs. S4 and S5). As expected, in LL, all three evening genes display a phase delay in the *rve* mutant (Supplemental Figs. S4 and S5). Both *PRR5* and *TOC1* have significantly decreased expression levels in the *rve* mutant when values are integrated across the LL time series (Supplemental Fig. S4). However, only *PRR5* shows an obvious decrease in peak levels of expression in *rve4 6 8* (Supplemental Fig. S4). We did not observe a significant difference in *LUX* expression levels in *rve4 6 8* (Supplemental Fig. S4). Thus, the overall increased levels of *PIF4* and *PIF5* expression in the *rve4 6 8* mutant in LL (Fig. 7) may be due to lower levels of PRR5 and/or TOC1.

We next examined *PRR5*, *TOC1*, and *LUX* expression in LD and SD conditions. Especially in LD conditions, there are clear differences in the waveforms and phases of expression of these evening genes in *rve4 6 8* (Fig. 5; Supplemental Fig. S4). However, quantification of their expression did not reveal significant decreases in expression in the *rve* mutant compared with the wild type when assessed across the entire LD and SD time series (Supplemental Fig. S4). Surprisingly, overall *TOC1* expression in LD time series is elevated slightly in the mutant compared with the wild type (Supplemental Fig. S4). These data suggest that the night-specific, but not overall, increases in *PIF4* and *PIF5* expression in *rve4 6 8* in LD and SD conditions (Fig. 7) may be due to changes in the phase of evening gene expression but are not attributable to changes in their overall expression levels. Together, these data suggest the RVEs have a key role in setting the appropriate phase of gene expression in light/dark cycles and overall target gene expression levels in constant environmental conditions.

The *PIFs* Are Epistatic to the *RVEs* at Multiple Growth Stages

The increased levels of *PIF4* and *PIF5* transcripts in *rve4 6 8* overall in LL and specifically at night in LD and SD conditions (Fig. 7) suggest that increased PIF activity might contribute to the enhanced growth phenotypes in this mutant. Therefore, we generated a quintuple *rve4 6 8 pif 4 5* mutant to investigate whether the *PIFs* are required for the large size phenotype of the *rve* mutants. As expected (Nozue et al., 2007; Lorrain et al., 2008), *pif4 5* double mutants have shorter hypocotyls than the wild type (Fig. 8). Notably, while the hypocotyls of the *rve4 6 8* mutant are almost 50% longer than those of the wild type in LL and LD conditions, the hypocotyls of the quintuple *rve4 6 8 pif4 5* mutant are almost the same length as those of the *pif4 5* mutant in these conditions (Fig. 8). A similar suppression of the *rve* hypocotyl phenotype is observed in plants grown in 12-h-light/12-h-dark conditions, both with and without sucrose in the growth medium (Supplemental Fig. S6). Interestingly, we did not observe epistasis when seedlings were maintained in SD conditions (Fig. 8). Loss of *rve4 6 8* in these conditions caused an ~50% increase in hypocotyl length in both the Col and *pif4 5* backgrounds. Thus, when seedlings are grown in LL, LD, or 12-h-light/12-h-dark conditions, PIF4 and/or PIF5 are largely responsible for the effects of *RVE4*, *RVE6*, and *RVE8* on hypocotyl growth; however, a different mechanism appears to cause the long hypocotyls of *rve4 6 8* seedlings grown in SD conditions.

We next sought to determine whether the *PIFs* are responsible for the large adult rosette phenotype in *rve* mutants. Therefore, we examined rosette and leaf size phenotypes of LD-grown quintuple *rve4 6 8 pif4 5* mutants and the appropriate controls at 3 weeks of age. Strikingly, the *pif4 5* and *rve4 6 8 pif4 5* mutants have very similar rosette diameters (Fig. 8). Consistent with this overall appearance, the blade areas, blade lengths, and petiole lengths of these mutants are not significantly different from each other (Fig. 8). Thus, the *pif4 5* mutations suppress both the seedling and adult growth phenotypes of *rve4 6 8* mutants, indicating a role for the RVEs in the modulation of *PIF* gene expression and the control of growth throughout plant development.

DISCUSSION

Numerous previous studies have highlighted the importance of the CCA1/LHY/RVE transcription factors in the plant circadian network (Wang and Tobin, 1998; Green and Tobin, 1999, 2002; Rawat et al., 2009, 2011; Farinas and Mas, 2011; Hsu et al., 2013) Remarkably, different members of this small gene family play contrasting roles: while CCA1 and LHY lengthen the circadian period (Green and Tobin, 1999; Alabadí et al., 2002; Mizoguchi et al., 2002) and RVE4, RVE6, and RVE8 shorten it (Farinas and Mas, 2011; Rawat et al., 2011; Hsu et al., 2013), RVE1 does not affect clock pace but instead mediates the circadian regulation of the auxin pathway (Rawat et al., 2009). With this range of functions in mind, we phenotyped plants mutant for *RVE3* and *RVE5*, the last two uncharacterized members of this Myb-like transcription factor family.

RVE8 and its close homologs *RVE4* and *RVE6* were shown previously to control circadian clock pace in a partially redundant manner (Hsu et al., 2013). We now show that the two remaining homologs of the *RVE8* clade, *RVE3* and *RVE5*, play only a minor role in controlling clock pace. The *rve3 5* double mutant has a free-running circadian period very similar to the wild type (Fig. 1). Additionally, although the free-running period of the *rve3 4 5 6 8* mutant is slightly longer than that of the triple *rve4 6 8* mutant in red plus blue light, the period differences are small (Fig. 1). Taken together, our results suggest that *RVE3* and *RVE5* only promote clock pace in conjunction with *RVE4*, *RVE6*, and *RVE8* and that their role in the clock is subtle. It is important to note that the *rve6* allele used in this study is not a complete knockout, retaining ~30% of normal *RVE6*

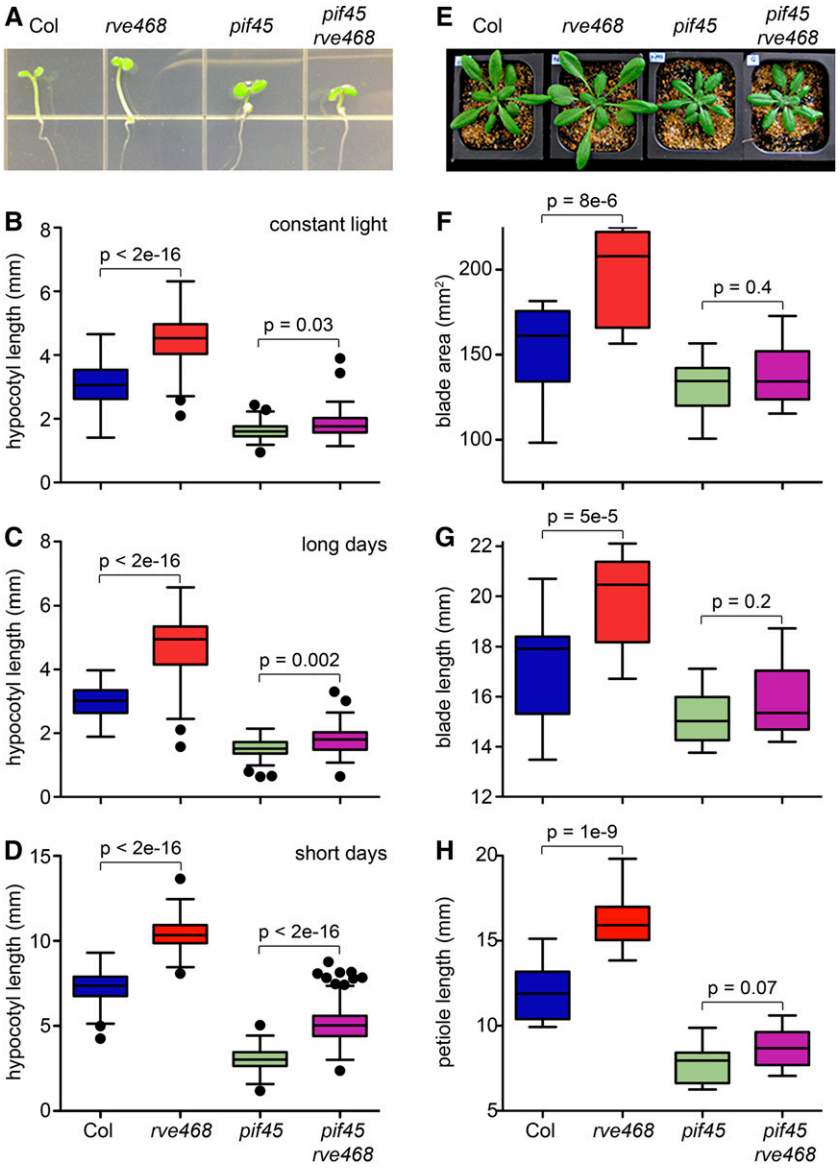

Figure 8. The *PIFs* are epistatic to the *RVEs* at both seedling and adult stages of development. A, Seedlings were grown in LL at 7.5 μmol m^{-2} s^{-1} (white light) for 6 d at 22°C. B, Quantification of hypocotyl length of plants grown as in A (n = 68–80). C and D, Seedlings were grown in LD cycles (C) or SD cycles (D) at 25 μmol m^{-2} s^{-1} (white light) on medium containing 3% sucrose for 6 d at 22°C, and hypocotyl length was measured (n = 72–92). E to H, Col, *rve4 6 8*, *pif4 5*, and *rve4 6 8 pif4 5* plants were grown in LD cycles (55 μmol m^{-2} s^{-1}) for 3 weeks. E, Three-week-old plants. F, Leaf 5 blade area. G, Blade length. H, Petiole length of the indicated genotypes of 3-week-old plants (n = 12). Lines within the box-and-whisker plots represent the medians; whiskers and outliers were plotted with the Tukey method. Significance is indicated as determined by a linear mixed-effect model with genotype as a fixed effect and replicate as a random effect. Error bars represent SE. Data shown are illustrative of at least two independent experiments.

transcript levels (Hsu et al., 2013). Further studies with a null *rve6* allele would reveal if the complete loss of all *RVE8* clade members affects rhythmic robustness in addition to causing a long-period phenotype.

In addition to longer free-running rhythms, the light regulation of clock function is altered in plants mutant for the *RVEs* (Fig. 1). Typically, the free-running circadian period of diurnal organisms is shorter at higher light intensities and longer at lower light intensities (Aschoff, 1960; Somers et al., 1998). In contrast to wild-type Arabidopsis, the circadian pace in *rve* triple and quintuple mutants is relatively insensitive to increasing fluence rates of red light (Fig. 1). Similar insensitivity to fluence rate is observed in plants expressing a constitutively activated phytochrome photoreceptor (Jones et al., 2015), suggesting that there are changes in red light input to the clock in *rve* mutants. Surprisingly, increasing intensities of continuous blue light result in the progressive lengthening of free-running period in the triple and quintuple *rve* mutants (Fig. 1). A similar lengthening of circadian period in response to increasing intensities of red (but not blue) light has been reported in plants mutant for *LNK1* or *LNK2* (Xie et al., 2014), which encode transcriptional coactivators that work with RVE proteins to control the expression of central clock genes (Rugnone et al., 2013; Xie et al., 2014). The differential sensitivities of *lnk* and *rve* mutants to red and blue light, therefore, are surprising at first. However, LNK1 and LNK2 affect clock function in a partially redundant manner (Rugnone et al., 2013; Xie et al., 2014), and the effect of light on clock pace in *lnk1 lnk2* mutants has not yet been reported. In addition, LNK proteins have been shown to antagonize RVE8 function in at least one clock output pathway (Pérez-García et al., 2015). Finally, LNK1 and LNK2 interact with CCA1 and LHY in addition to RVE4 and RVE8

(Xie et al., 2014), suggesting that they may affect the clock independent of RVE8 clade proteins. Therefore, the relationship between the Myb-like transcription factors and the LNK proteins is complex, making mutant phenotypes difficult to predict.

The most obvious phenotype in the *rve* triple and quintuple mutants is their enhanced size relative to the wild type at both seedling and adult stages of development (Figs. 3 and 4). *RVE3* and *RVE5* appear to play a minor role in growth regulation, as the triple and quintuple *rve* mutants have similar growth phenotypes. One exception is the longer petiole lengths of *rve3 4 5 6 8* plants relative to *rve4 6 8* plants at 3 weeks of age; interestingly, this difference is observed for plants grown in SD conditions but not those grown in LD conditions (Supplemental Fig. S2). Therefore, *RVE3* and *RVE5* play both photoperiod- and tissue-specific roles in growth regulation.

Epistasis experiments also suggest that RVE4, RVE6, and RVE8 regulate plant growth via distinct mechanisms depending upon the photoperiod. *PIF4* and/or *PIF5* are required for the enhanced growth of *rve* triple mutants in most photoperiods, but not in SD conditions (Fig. 8; Supplemental Fig. S6). It is possible that the enhanced growth of *rve4 6 8* mutants in SD conditions is due instead to misregulation of the related transcription factors PIF1 and/or PIF3. Both of these proteins have been implicated in the promotion of hypocotyl elongation in response to SD conditions (Soy et al., 2012, 2014). Moreover, when plants are grown in SD conditions, TOC1 and PIF3 coregulate the expression of growth-related genes, with TOC1 inhibiting PIF transactivation activity at the promoters of common target genes in the first part of the night (Soy et al., 2016). It is possible that, in *rve4 6 8* plants grown in SD conditions, there is a delay in the phase of TOC1 protein accumulation such that the normal inhibition of PIF growth-promoting activity during the early night does not occur.

In contrast to plants grown in SD conditions, the enhanced growth of *rve4 6 8* mutants maintained in LL, LD, or 12-h-light/12-h-dark conditions depends on functional *PIF4* and *PIF5* genes (Fig. 8; Supplemental Fig. S6). In addition, the overall expression levels of both *PIF4* and *PIF5* in the *rve* mutant are elevated significantly relative to wild-type plants when examined over a 1.5-d time course collected in LL (Fig. 7). RVE8 directly promotes the expression of *PRR5* and *TOC1* (Rawat et al., 2011; Hsu et al., 2013), two known repressors of *PIF4* and *PIF5* expression (Kunihiro et al., 2011; Huang et al., 2012; Nakamichi et al., 2012). Notably, we find that *PRR5* and *TOC1* expression is reduced significantly in *rve4 6 8* plants grown in LL (Supplemental Fig. S4), potentially explaining the enhanced expression of *PIF4* and *PIF5* in this condition.

The ability of the *pif4 5* mutations to suppress the long-hypocotyl phenotypes of *rve* mutants in LL (Fig. 8) is surprising at first, given the relatively small increases in *PIF4* and *PIF5* transcript levels in *rve4 6 8* plants (Fig. 7). However, previous studies have demonstrated that modest increases in trough levels of *PIF4* and *PIF5* transcripts cause increased hypocotyl elongation (Nusinow et al., 2011; Wang et al., 2015).

In LL conditions, growth phenotypes in *rve4 6 8* cannot be attributed to conflicts of the circadian phase with light/dark transitions. However, the same is not true in LD conditions. In this condition, we find that *PIF4* and *PIF5* expression levels are increased significantly during the dark period (Fig. 7), although not across the entire time series (data not shown). Since PIF proteins are stable in the dark but not in the light (Nozue et al., 2007; Lorrain et al., 2008), the night-phased up-regulation of these transcripts is likely to lead to a greater accumulation of PIF proteins in *rve4 6 8* than in the wild type. PIF4 and PIF5 proteins induce the expression of genes that positively regulate hypocotyl growth (Franklin et al., 2011; Kunihiro et al., 2011; Nozue et al., 2011; Hornitschek et al., 2012; Sun et al., 2012), suggesting a mechanism to explain the enhanced growth in *rve4 6 8* plants in LD conditions. Indeed, under this photoperiod, *pif4 5* is epistatic to *rve4 6 8* at both the seedling and rosette (Fig. 8) stages of development. Together, these data strongly suggest that the growth phenotypes of *rve4 6 8* in LD conditions are due to elevated *PIF4* and/or *PIF5* expression levels at night.

These increased nighttime expression levels of *PIF4* and *PIF5* in LD conditions may be attributed both to a delay in circadian phase (given the long-period phenotype of *rve4 6 8*) and to increased trough levels of the transcripts (Fig. 7). Thus, we conclude that, in LD cycles, the *rve4 6 8* growth phenotypes are due to alterations in *PIF4* and/or *PIF5* expression that are caused by both direct RVE control of gene expression and the overall long-period phenotype of this mutant.

Recent work has highlighted the importance of both shared and separate molecular pathways controlling growth at different stages of development and in different environmental conditions (Nozue et al., 2015; Seaton et al., 2015). Our results here show that *RVE4*, *RVE6*, and *RVE8* are partially redundant inhibitors of plant growth throughout plant development and that both juvenile and adult growth phenotypes of *rve* mutants require PIF4 and/or PIF5 function (Fig. 8; Supplemental Fig. S6). These data strongly suggest that these PIFs enhance not only hypocotyl growth but also the growth of adult plants. This PIF-dependent promotion of leaf growth at the adult stages of plant development is surprising given previous reports that both loss of function and constitutive overexpression of *PIF4/PIF5* reduce adult plant size (Fujimori et al., 2004; Lorrain et al., 2008; Keller et al., 2011; Kumar et al., 2012; Nieto et al., 2015; Nozue et al., 2015). The PIF-mediated promotion of adult growth in *rve4 6 8* may be due to either the modest increases or the precise time of day at which *PIF4/PIF5* expression is increased.

The perturbation of clock genes is generally associated with a reduction in adult biomass (Dodd et al., 2005; Graf et al., 2010). Other reported cases in which the mutation of clock genes increases adult plant size can be attributed to a delay in flowering time rather

than to growth promotion per se. For example, plants overexpressing *CCA1* or mutant for *PRR5*, *PRR7*, and *PRR9* display reduced growth rates as juveniles (Ruts et al., 2012) but flower very late (Wang and Tobin, 1998; Nakamichi et al., 2005b) and, thus, are very large at the time of senescence. To our knowledge, the enhanced growth rate we observe in *rve8* clade mutants has not been reported previously for a circadian mutant.

The increased size phenotypes of the *rve* triple and quintuple mutants might be immediately relevant for agricultural purposes. Phylogenetic analysis shows that the *RVE8* clade is conserved in both monocot and dicot crop species (Supplemental Fig. S7). Recent studies show that variants in a number of clock gene homologs in crop species, including homologs of genes that are RVE8 targets in Arabidopsis, are associated with favorable yield traits (Bendix et al., 2015). Perturbations in the circadian clock have been associated with the growth advantages seen in polyploids and in hybrids (Ni et al., 2009). Intriguingly, evening element motifs are enriched in the promoters of genes specifically up-regulated in polyploids (Ni et al., 2009). Together with our demonstration of enhanced growth rates in *rve* mutants, this suggests that modulation of RVE8 function may contribute to the hybrid vigor previously associated with alterations in CCA1 and LHY function (Chen, 2010).

MATERIALS AND METHODS

Mutant Alleles and Genotyping

Arabidopsis (*Arabidopsis thaliana*) Col, *CCR2*::*LUC* wild type, and the *rve 4 6 8*; *CCR2*::*LUC* mutant lines were described previously (Rawat et al., 2011; Hsu et al., 2013) The quintuple *rve* mutant was generated by introgressing the *rve3-1* allele (SALK_001480C) and a *rve5-1* mutant allele (SAIL_769_A09) into the previously characterized *rve4 6 8* triple mutant (Hsu et al., 2013). Genotypic verification of combinatorial mutants was performed via PCR analysis using primers as follows: *RVE3* WT, 5′-CAACAACGATACCGGTTTCCATACG-3′ and 5′-TCGCAATGCACTAATCCATGCTTAC-3′; *RVE3* TDNA, 5′-CAACAACGATACCGGTTTCCATACG-3′ and 5′-GCGTGGACCGCTTGCTGCAACT-3′; *RVE5* WT, 5′-TCTGGGTACTAGAGCAACGAGAC-3′ and 5′-ACTCCCGGTTCCTCTACTATCAC-3′; and *RVE5* TDNA, 5′-TAGCATCTGAATTTCATAACCAATCTCGATACAC-3′ and 5′-ACTCCCGGTTCCTCTACTATCAC-3′. The primers used to genotype *RVE4*, *RVE6*, and *RVE8* were described previously (Rawat et al., 2011; Hsu et al., 2013). The quantitative PCR primers used to examine *RVE3* expression are 5′-AGCCCTTCATCTATTTGACCGGGA-3′ and 5′-TGTGCGTGGCTTCGTATCTGTATC-3′. The primers used to quantify *RVE5* expression via semiquantitative reverse transcription-PCR are 5′-ATGGTGTCCGTAAACCCTAGAC-3′ and 5′-CTATTTCAAAGCTTTAGCGCTGTA-3′. The double *pif4* 5 mutant (*pif4-101* [GARLIC_114_G06] and *pif5-1* [SALK_087012]; Fujimori et al., 2004; Lorrain et al., 2008) was crossed to the *rve4 6 8* mutant to generate the *rve4 6 8 pif4 5* quintuple mutant. The primers used to genotype the PIF4 and PIF5 alleles are as follows: *PIF4* WT, 5′-CTCGATTTCCGGTTATGG-3′ and 5′-CAGACGGTTGATCATCTG-3′; *PIF4* TDNA, 5′-CAGACGGTTGATCATCTG-3′ and 5′-GCATCTGAATTTCATAACCAATC-3′; *PIF5* WT, 5′-TCGCTCACTCGCTTACTTAC-3′ and 5′-TCTCTACGAGCTTGGCTTTG-3′; and *PIF5* TDNA, 5′-TCGCTCACTCGCTTACTTAC-3′ and 5′-GGCAATCAGCTGTTGCCCGTCTCACTGGTG-3′. The primers used to amplify the wild-type and T-DNA-specific bands for *RVE4*, *RVE6*, and *RVE8* have been reported previously (Hsu et al., 2013).

Circadian Period Analysis

Seeds were sown on petri plates containing 1× Murashige and Skoog (MS) medium (Sigma-Aldrich), 3% sucrose, and 0.8% agar. Seeds were then stratified for 2 to 4 d in the dark at 4°C before entrainment in 12-h-light/12-h-dark conditions for 6 d at 50 μmol m^{-2} s^{-1} white light and 22°C. Seedlings were sprayed with 3 mM D-luciferin (Biosynth), and luciferase activity was detected using an ORCA II ER CCD (Hamamatsu Photonics) with illumination provided by light-emitting diode SnapLites (Quantum Devices) emitting continuous monochromatic red or blue light. Neutral density filters (Rosco Laboratories) were used to generate variable light fluence rates. Bioluminescence was quantified using MetaMorph software (Molecular Devices), and period analysis was performed using the Biological Rhythms Analysis Software System (http://millar.bio.ed.ac.uk/PEBrown/BRASS/BrassPage.htm).

Hypocotyl Analysis

Seeds were plated on medium containing 1× MS salts, 0.8% agar, and concentrations of sucrose ranging from 0% to 6% (w/v) as indicated. Seeds were stratified and released to the appropriate daylength conditions under cool-white fluorescent bulbs at the indicated light intensities, at 22°C, for 7 d. Neutral density filters were utilized to generate the indicated fluence rates. Individual hypocotyls were transferred to transparencies and scanned following established protocols (http://malooflab.openwetware.org/Hypocotyl_measurement.html). Hypocotyl lengths were measured using ImageJ (http://imagej.nih.gov/ij/).

Adult Plant Phenotyping and Flowering Time Analysis

Arabidopsis seeds were plated on 0.5× MS medium with 0.8% agar medium and cold stratified for 2 to 4 d before being transferred to growth chambers illuminated with cool-white fluorescent bulbs at 50 μmol m^{-2} s^{-1} white light, at 22°C, for 4 d. Upon germination, seedlings were transferred directly to soil and grown under 50 μmol m^{-2} s^{-1} white light, at 22°C, in LD conditions (16 h of light/8 h of dark) for the indicated lengths of time. Three- and 6-week-old plant leaves were analyzed according to the LeafJ protocol (Maloof et al., 2013). Rosette growth was determined manually using calipers to measure the distance between the eighth and ninth leaves of every plant. Total aerial biomass was quantified for 6-week-old plants after they had been stored and dried for 3 d at 40°C. Flowering time was scored when plants generated a 1-cm bolt in LD conditions.

Cell Size Analysis

Six-week-old plants were dissected, and leaves 8 and 9 were fixed and cleared according to previously described methods (Tsuge et al., 1996; Horiguchi et al., 2006) for 2 to 3 h. Cleared leaves were imaged at 20× magnification using a Zeiss Axioscop 2 plus microscope, and mesophyll cell area was determined using ImageJ software (http://imagej.nih.gov/ij/).

RNA Extraction and qRT-PCR Analysis

Seedlings were grown for 6 d in 12-h-light/12-h-dark conditions and then released to LL for 32 h before ~20 to 40 seedlings were collected per sample for the LL time course. For the LD and SD time courses, seedlings were grown in 16-h-light/8-h-dark or 8-h-light/16-h-dark photocycles for 6 d before sample collection was started. RNA was extracted from whole seedlings using Trizol reagent following the manufacturer's protocol (Life Technologies). RNA was subjected to DNase treatment following the Qiagen RNase-free DNase protocol, and cDNA was synthesized using oligo(dT) primers and SuperScript II Reverse Transcriptase (Life Technologies). qRT-PCR analysis was performed with reagents as described previously (Martin-Tryon and Harmer, 2008) using a Bio-Rad iQ5 thermocycler. Data were analyzed by the delta Ct method using iCycler iQ Optical Systems Software version 3.1 (Bio-Rad Laboratories). Gene expression analysis was conducted using previously described primers (Nusinow et al., 2011; Hsu et al., 2013). Quantification of gene expression across the LL, LD, and SD time series was carried out by computing the area under the curves using natural cubic spline interpolation using the auc function in the MESS package (Ekstrøm, 2016) in the R statistical environment (R Core Team, 2016). Statistical significance was then assessed with linear mixed-effect models with genotype as a fixed effect and replicate as a random effect using the R packages lme4 (Bates et al., 2015) and lmerTest (Kuznetsova et al., 2016).

Phylogenetic Analysis

Phylogenetic analysis was performed on the Phylogeny.fr platform (Dereeper et al., 2008). Amino acid sequences for Myb-like factors were aligned

with MUSCLE (version 3.8.31) configured for highest accuracy (default settings). The phylogenetic tree was reconstructed using the maximum likelihood method implemented in the PhyML program (version 3.1/3.0 aLRT). The WAG substitution model was selected assuming an estimated proportion of invariant sites (of 0.039) and four γ-distributed rate categories to account for rate heterogeneity across sites. The γ shape parameter was estimated directly from the data ($\gamma = 1.046$). Reliability for the internal branch was assessed using the aLRT test (SH-Like). Graphical representation and editing of the phylogenetic tree were performed with TreeDyn (version 198.3).

Accession Numbers

UniProtKB/Swiss-Prot reference sequence numbers are as follows: for Arabidopsis: At_CCA1 (P92973), At_LHY (Q6R0H1), At_RVE1 (F4KGY6), At_RVE2 (F4K5X6), At_RVE3 (Q6R0H0), At_RVE4 (Q6R0G4), At_RVE5 (C0SVG5), At_RVE6 (Q8H0W3), At_RVE7 (B3H5A8), At_RVE7-like (F4J2J6), and At_RVE8 (Q8RWU3); for rice (*Oryza sativa*): Os_01g06320 (Q5ZCD7), Os_02g45670 (B9F1T8), Os_02g46030 (Q6ZHD2), Os_04g49450 (A3AWS7), Os_05g07010 (C7J2V5), Os_06g01670 (Q5VS69), Os_06g45840 (B9FQF0), Os_06g51260 (B5AEI9), and Os_08g06110 (Q0J7W9); for tomato (*Solanum lycopersicum*): Sl_01g095030 (K4AZP3), Sl_02g036370 (K4B5T0), Sl_03g098320 (K4BJP7), Sl_06g036300 (K4C4Z7), Sl_10g005080 (K4CX41), and Sl_10g084370 (K4D3M3).

Supplemental Data

The following supplemental materials are available.

Supplemental Figure S1. Gene expression in *rve3* and *rve5* mutants.

Supplemental Figure S2. Aerial growth phenotypes of 3-week-old wild-type and *rve* mutant plants grown in long or short days.

Supplemental Figure S3. *PIF4* and *PIF5* expression is elevated in *rve4 6 8* mutants (data graphed using linear scale).

Supplemental Figure S4. *PRR5, TOC1,* and *LUX* expression is altered in *rve4 6 8* mutants (data graphed using log scale).

Supplemental Figure S5. *PRR5, TOC1,* and *LUX* expression is altered in *rve4 6 8* mutants.

Supplemental Figure S6. The *PIFs* are epistatic to the *RVEs* when grown on medium lacking sucrose.

Supplemental Figure S7. The *RVE8* clade is conserved in monocot and dicot species.

ACKNOWLEDGMENTS

We thank the Arabidopsis Biological Resource Center and Kazunari Nozue for providing seeds as well as members of the Harmer laboratory, Kazunari Nozue, and Julin Maloof for helpful discussions.

Received January 30, 2017; accepted February 28, 2017; published March 2, 2017.

LITERATURE CITED

Alabadí D, Yanovsky MJ, Más P, Harmer SL, Kay SA (2002) Critical role for CCA1 and LHY in maintaining circadian rhythmicity in Arabidopsis. Curr Biol **12:** 757–761

Aschoff J (1960) Exogenous and endogenous components in circadian rhythms. Cold Spring Harb Symp Quant Biol **25:** 11–28

Bates D, Maechler M, Bolker B, Walker S (2015) Fitting linear mixed-effects models using lme4. J Stat Softw **67:** 1–48

Bendix C, Marshall CM, Harmon FG (2015) Circadian clock genes universally control key agricultural traits. Mol Plant **8:** 1135–1152

Chen ZJ (2010) Molecular mechanisms of polyploidy and hybrid vigor. Trends Plant Sci **15:** 57–71

Covington MF, Maloof JN, Straume M, Kay SA, Harmer SL (2008) Global transcriptome analysis reveals circadian regulation of key pathways in plant growth and development. Genome Biol **9:** R130

de Lucas M, Davière JM, Rodríguez-Falcón M, Pontin M, Iglesias-Pedraz JM, Lorrain S, Fankhauser C, Blázquez MA, Titarenko E, Prat S (2008) A molecular framework for light and gibberellin control of cell elongation. Nature **451:** 480–484

Dereeper A, Guignon V, Blanc G, Audic S, Buffet S, Chevenet F, Dufayard JF, Guindon S, Lefort V, Lescot M, et al (2008) Phylogeny.fr: robust phylogenetic analysis for the non-specialist. Nucleic Acids Res **36:** W465–W469

Devlin PF, Kay SA (2000) Cryptochromes are required for phytochrome signaling to the circadian clock but not for rhythmicity. Plant Cell **12:** 2499–2510

Dixon LE, Knox K, Kozma-Bognar L, Southern MM, Pokhilko A, Millar AJ (2011) Temporal repression of core circadian genes is mediated through EARLY FLOWERING 3 in Arabidopsis. Curr Biol **21:** 120–125

Dodd AN, Salathia N, Hall A, Kévei E, Tóth R, Nagy F, Hibberd JM, Millar AJ, Webb AA (2005) Plant circadian clocks increase photosynthesis, growth, survival, and competitive advantage. Science **309:** 630–633

Dornbusch T, Michaud O, Xenarios I, Fankhauser C (2014) Differentially phased leaf growth and movements in *Arabidopsis* depend on coordinated circadian and light regulation. Plant Cell **26:** 3911–3921

Doyle MR, Davis SJ, Bastow RM, McWatters HG, Kozma-Bognár L, Nagy F, Millar AJ, Amasino RM (2002) The ELF4 gene controls circadian rhythms and flowering time in Arabidopsis thaliana. Nature **419:** 74–77

Dunlap JC (1999) Molecular bases for circadian clocks. Cell **96:** 271–290

Ekstrøm C (2016) MESS: Miscellaneous Esoteric Statistical Scripts. R package version 0.4-3. https://CRAN.R-project.org/package=MESS

Farinas B, Mas P (2011) Functional implication of the MYB transcription factor RVE8/LCL5 in the circadian control of histone acetylation. Plant J **66:** 318–329

Farré EM (2012) The regulation of plant growth by the circadian clock. Plant Biol (Stuttg) **14:** 401–410

Franklin KA, Lee SH, Patel D, Kumar SV, Spartz AK, Gu C, Ye S, Yu P, Breen G, Cohen JD, et al (2011) Phytochrome-interacting factor 4 (PIF4) regulates auxin biosynthesis at high temperature. Proc Natl Acad Sci USA **108:** 20231–20235

Fujimori T, Yamashino T, Kato T, Mizuno T (2004) Circadian-controlled basic/helix-loop-helix factor, PIL6, implicated in light-signal transduction in Arabidopsis thaliana. Plant Cell Physiol **45:** 1078–1086

Gendron JM, Pruneda-Paz JL, Doherty CJ, Gross AM, Kang SE, Kay SA (2012) Arabidopsis circadian clock protein, TOC1, is a DNA-binding transcription factor. Proc Natl Acad Sci USA **109:** 3167–3172

Gong W, He K, Covington M, Dinesh-Kumar SP, Snyder M, Harmer SL, Zhu YX, Deng XW (2008) The development of protein microarrays and their applications in DNA-protein and protein-protein interaction analyses of Arabidopsis transcription factors. Mol Plant **1:** 27–41

Goodspeed D, Chehab EW, Min-Venditti A, Braam J, Covington MF (2012) Arabidopsis synchronizes jasmonate-mediated defense with insect circadian behavior. Proc Natl Acad Sci USA **109:** 4674–4677

Graf A, Schlereth A, Stitt M, Smith AM (2010) Circadian control of carbohydrate availability for growth in Arabidopsis plants at night. Proc Natl Acad Sci USA **107:** 9458–9463

Green RM, Tingay S, Wang ZY, Tobin EM (2002) Circadian rhythms confer a higher level of fitness to Arabidopsis plants. Plant Physiol **129:** 576–584

Green RM, Tobin EM (1999) Loss of the circadian clock-associated protein 1 in Arabidopsis results in altered clock-regulated gene expression. Proc Natl Acad Sci USA **96:** 4176–4179

Green RM, Tobin EM (2002) The role of CCA1 and LHY in the plant circadian clock. Dev Cell **2:** 516–518

Harmer SL (2009) The circadian system in higher plants. Annu Rev Plant Biol **60:** 357–377

Harmer SL, Kay SA (2005) Positive and negative factors confer phase-specific circadian regulation of transcription in *Arabidopsis*. Plant Cell **17:** 1926–1940

Harmer SL, Panda S, Kay SA (2001) Molecular bases of circadian rhythms. Annu Rev Cell Dev Biol **17:** 215–253

Hazen SP, Schultz TF, Pruneda-Paz JL, Borevitz JO, Ecker JR, Kay SA (2005) LUX ARRHYTHMO encodes a Myb domain protein essential for circadian rhythms. Proc Natl Acad Sci USA **102:** 10387–10392

Helfer A, Nusinow DA, Chow BY, Gehrke AR, Bulyk ML, Kay SA (2011) LUX ARRHYTHMO encodes a nighttime repressor of circadian gene expression in the Arabidopsis core clock. Curr Biol **21:** 126–133

Hicks KA, Albertson TM, Wagner DR (2001) EARLY FLOWERING3 encodes a novel protein that regulates circadian clock function and flowering in *Arabidopsis*. Plant Cell **13:** 1281–1292

Horiguchi G, Fujikura U, Ferjani A, Ishikawa N, Tsukaya H (2006) Large-scale histological analysis of leaf mutants using two simple leaf observation methods: identification of novel genetic pathways governing the size and shape of leaves. Plant J **48:** 638–644

Hornitschek P, Kohnen MV, Lorrain S, Rougemont J, Ljung K, López-Vidriero I, Franco-Zorrilla JM, Solano R, Trevisan M, Pradervand S, et al (2012) Phytochrome interacting factors 4 and 5 control seedling growth in changing light conditions by directly controlling auxin signaling. Plant J **71:** 699–711

Hsu PY, Devisetty UK, Harmer SL (2013) Accurate timekeeping is controlled by a cycling activator in Arabidopsis. eLife **2:** e00473

Hsu PY, Harmer SL (2014) Wheels within wheels: the plant circadian system. Trends Plant Sci **19:** 240–249

Huang W, Pérez-García P, Pokhilko A, Millar AJ, Antoshechkin I, Riechmann JL, Mas P (2012) Mapping the core of the Arabidopsis circadian clock defines the network structure of the oscillator. Science **336:** 75–79

Iijima M, Matsushita N (2011) A circadian and an ultradian rhythm are both evident in root growth of rice. J Plant Physiol **168:** 2072–2080

Jones MA, Hu W, Litthauer S, Lagarias JC, Harmer SL (2015) A constitutively active allele of phytochrome B maintains circadian robustness in the absence of light. Plant Physiol **169:** 814–825

Keller MM, Jaillais Y, Pedmale UV, Moreno JE, Chory J, Ballaré CL (2011) Cryptochrome 1 and phytochrome B control shade-avoidance responses in Arabidopsis via partially independent hormonal cascades. Plant J **67:** 195–207

Koini MA, Alvey L, Allen T, Tilley CA, Harberd NP, Whitelam GC, Franklin KA (2009) High temperature-mediated adaptations in plant architecture require the bHLH transcription factor PIF4. Curr Biol **19:** 408–413

Kumar SV, Lucyshyn D, Jaeger KE, Alós E, Alvey E, Harberd NP, Wigge PA (2012) Transcription factor PIF4 controls the thermosensory activation of flowering. Nature **484:** 242–245

Kunihiro A, Yamashino T, Nakamichi N, Niwa Y, Nakanishi H, Mizuno T (2011) Phytochrome-interacting factor 4 and 5 (PIF4 and PIF5) activate the homeobox ATHB2 and auxin-inducible IAA29 genes in the coincidence mechanism underlying photoperiodic control of plant growth of Arabidopsis thaliana. Plant Cell Physiol **52:** 1315–1329

Kuznetsova A, Brockhoff PB, Christensen RHB (2016) lmerTest: Tests in Linear Mixed Effects Models. R package version 2.0-30. https://CRAN.R-project.org/package=lmerTest

Lastdrager J, Hanson J, Smeekens S (2014) Sugar signals and the control of plant growth and development. J Exp Bot **65:** 799–807

Leivar P, Monte E, Oka Y, Liu T, Carle C, Castillon A, Huq E, Quail PH (2008) Multiple phytochrome-interacting bHLH transcription factors repress premature seedling photomorphogenesis in darkness. Curr Biol **18:** 1815–1823

Leivar P, Tepperman JM, Cohn MM, Monte E, Al-Sady B, Erickson E, Quail PH (2012) Dynamic antagonism between phytochromes and PIF family basic helix-loop-helix factors induces selective reciprocal responses to light and shade in a rapidly responsive transcriptional network in *Arabidopsis*. Plant Cell **24:** 1398–1419

Liu Z, Zhang Y, Liu R, Hao H, Wang Z, Bi Y (2011) Phytochrome interacting factors (PIFs) are essential regulators for sucrose-induced hypocotyl elongation in Arabidopsis. J Plant Physiol **168:** 1771–1779

Lorrain S, Allen T, Duek PD, Whitelam GC, Fankhauser C (2008) Phytochrome-mediated inhibition of shade avoidance involves degradation of growth-promoting bHLH transcription factors. Plant J **53:** 312–323

Maloof JN, Nozue K, Mumbach MR, Palmer CM (2013) LeafJ: an ImageJ plugin for semi-automated leaf shape measurement. J Vis Exp 71 50028

Martin-Tryon EL, Harmer SL (2008) XAP5 CIRCADIAN TIMEKEEPER coordinates light signals for proper timing of photomorphogenesis and the circadian clock in *Arabidopsis*. Plant Cell **20:** 1244–1259

McClung CR (2014) Wheels within wheels: new transcriptional feedback loops in the Arabidopsis circadian clock. F1000Prime Rep **6:** 2

Mizoguchi T, Wheatley K, Hanzawa Y, Wright L, Mizoguchi M, Song HR, Carré IA, Coupland G (2002) LHY and CCA1 are partially redundant genes required to maintain circadian rhythms in Arabidopsis. Dev Cell **2:** 629–641

Mizuno T, Kitayama M, Oka H, Tsubouchi M, Takayama C, Nomoto Y, Yamashino T (2014) The EC night-time repressor plays a crucial role in modulating circadian clock transcriptional circuitry by conservatively double-checking both warm-night and night-time-light signals in a synergistic manner in Arabidopsis thaliana. Plant Cell Physiol **55:** 2139–2151

Nagel DH, Doherty CJ, Pruneda-Paz JL, Schmitz RJ, Ecker JR, Kay SA (2015) Genome-wide identification of CCA1 targets uncovers an expanded clock network in Arabidopsis. Proc Natl Acad Sci USA **112:** E4802–E4810

Nakamichi N, Kiba T, Kamioka M, Suzuki T, Yamashino T, Higashiyama T, Sakakibara H, Mizuno T (2012) Transcriptional repressor PRR5 directly regulates clock-output pathways. Proc Natl Acad Sci USA **109:** 17123–17128

Nakamichi N, Kita M, Ito S, Yamashino T, Mizuno T (2005b) PSEUDO-RESPONSE REGULATORS, PRR9, PRR7 and PRR5, together play essential roles close to the circadian clock of Arabidopsis thaliana. Plant Cell Physiol **46:** 686–698

Ni Z, Kim ED, Ha M, Lackey E, Liu J, Zhang Y, Sun Q, Chen ZJ (2009) Altered circadian rhythms regulate growth vigour in hybrids and allopolyploids. Nature **457:** 327–331

Nieto C, López-Salmerón V, Davière JM, Prat S (2015) ELF3-PIF4 interaction regulates plant growth independently of the evening complex. Curr Biol **25:** 187–193

Nomoto Y, Kubozono S, Miyachi M, Yamashino T, Nakamichi N, Mizuno T (2012) A circadian clock- and PIF4-mediated double coincidence mechanism is implicated in the thermosensitive photoperiodic control of plant architectures in Arabidopsis thaliana. Plant Cell Physiol **53:** 1965–1973

Nozue K, Covington MF, Duek PD, Lorrain S, Fankhauser C, Harmer SL, Maloof JN (2007) Rhythmic growth explained by coincidence between internal and external cues. Nature **448:** 358–361

Nozue K, Harmer SL, Maloof JN (2011) Genomic analysis of circadian clock-, light-, and growth-correlated genes reveals PHYTOCHROME-INTERACTING FACTOR5 as a modulator of auxin signaling in Arabidopsis. Plant Physiol **156:** 357–372

Nozue K, Tat AV, Kumar Devisetty U, Robinson M, Mumbach MR, Ichihashi Y, Lekkala S, Maloof JN (2015) Shade avoidance components and pathways in adult plants revealed by phenotypic profiling. PLoS Genet **11:** e1004953

Nusinow DA, Helfer A, Hamilton EE, King JJ, Imaizumi T, Schultz TF, Farré EM, Kay SA (2011) The ELF4-ELF3-LUX complex links the circadian clock to diurnal control of hypocotyl growth. Nature **475:** 398–402

Pérez-García P, Ma Y, Yanovsky MJ, Mas P (2015) Time-dependent sequestration of RVE8 by LNK proteins shapes the diurnal oscillation of anthocyanin biosynthesis. Proc Natl Acad Sci USA **112:** 5249–5253

Poiré R, Wiese-Klinkenberg A, Parent B, Mielewczik M, Schurr U, Tardieu F, Walter A (2010) Diel time-courses of leaf growth in monocot and dicot species: endogenous rhythms and temperature effects. J Exp Bot **61:** 1751–1759

Pokhilko A, Fernández AP, Edwards KD, Southern MM, Halliday KJ, Millar AJ (2012) The clock gene circuit in Arabidopsis includes a repressilator with additional feedback loops. Mol Syst Biol **8:** 574

R Core Team R (2016) R: A Language and Environment for Statistical Computing. R Foundation for Statistical Computing, Vienna. https://www.R-project.org/

Rawat R, Schwartz J, Jones MA, Sairanen I, Cheng Y, Andersson CR, Zhao Y, Ljung K, Harmer SL (2009) REVEILLE1, a Myb-like transcription factor, integrates the circadian clock and auxin pathways. Proc Natl Acad Sci USA **106:** 16883–16888

Rawat R, Takahashi N, Hsu PY, Jones MA, Schwartz J, Salemi MR, Phinney BS, Harmer SL (2011) REVEILLE8 and PSEUDO-REPONSE REGULATOR5 form a negative feedback loop within the Arabidopsis circadian clock. PLoS Genet **7:** e1001350

Rugnone ML, Faigón Soverna A, Sanchez SE, Schlaen RG, Hernando CE, Seymour DK, Mancini E, Chernomoretz A, Weigel D, Más P, et al (2013) LNK genes integrate light and clock signaling networks at the core of the Arabidopsis oscillator. Proc Natl Acad Sci USA **110:** 12120–12125

Ruts T, Matsubara S, Wiese-Klinkenberg A, Walter A (2012) Aberrant temporal growth pattern and morphology of root and shoot caused by a defective circadian clock in Arabidopsis thaliana. Plant J **72:** 154–161

Schaffer R, Ramsay N, Samach A, Corden S, Putterill J, Carré IA, Coupland G (1998) The late elongated hypocotyl mutation of Arabidopsis disrupts circadian rhythms and the photoperiodic control of flowering. Cell **93:** 1219–1229

Seaton DD, Smith RW, Song YH, MacGregor DR, Stewart K, Steel G, Foreman J, Penfield S, Imaizumi T, Millar AJ, et al (2015) Linked circadian outputs control elongation growth and flowering in response to photoperiod and temperature. Mol Syst Biol **11:** 776

Somers DE, Devlin PF, Kay SA (1998) Phytochromes and cryptochromes in the entrainment of the Arabidopsis circadian clock. Science **282:** 1488–1490

Song YH, Ito S, Imaizumi T (2013) Flowering time regulation: photoperiod- and temperature-sensing in leaves. Trends Plant Sci **18:** 575–583

Soy J, Leivar P, González-Schain N, Martín G, Diaz C, Sentandreu M, Al-Sady B, Quail PH, Monte E (2016) Molecular convergence of clock and photosensory pathways through PIF3-TOC1 interaction and co-occupancy of target promoters. Proc Natl Acad Sci USA **113:** 4870–4875

Soy J, Leivar P, González-Schain N, Sentandreu M, Prat S, Quail PH, Monte E (2012) Phytochrome-imposed oscillations in PIF3 protein abundance regulate hypocotyl growth under diurnal light/dark conditions in Arabidopsis. Plant J **71:** 390–401

Soy J, Leivar P, Monte E (2014) PIF1 promotes phytochrome-regulated growth under photoperiodic conditions in Arabidopsis together with PIF3, PIF4, and PIF5. J Exp Bot **65:** 2925–2936

Stavang JA, Gallego-Bartolomé J, Gómez MD, Yoshida S, Asami T, Olsen JE, García-Martínez JL, Alabadí D, Blázquez MA (2009) Hormonal regulation of temperature-induced growth in Arabidopsis. Plant J **60:** 589–601

Stewart JL, Maloof JN, Nemhauser JL (2011) PIF genes mediate the effect of sucrose on seedling growth dynamics. PLoS ONE **6:** e19894

Sun J, Qi L, Li Y, Chu J, Li C (2012) PIF4-mediated activation of YUCCA8 expression integrates temperature into the auxin pathway in regulating Arabidopsis hypocotyl growth. PLoS Genet **8:** e1002594

Tsuge T, Tsukaya H, Uchimiya H (1996) Two independent and polarized processes of cell elongation regulate leaf blade expansion in Arabidopsis thaliana (L.) Heynh. Development **122:** 1589–1600

Wang CQ, Sarmast MK, Jiang J, Dehesh K (2015) The transcriptional regulator BBX19 promotes hypocotyl growth by facilitating COP1-mediated EARLY FLOWERING3 degradation in *Arabidopsis*. Plant Cell **27:** 1128–1139

Wang ZY, Tobin EM (1998) Constitutive expression of the CIRCADIAN CLOCK ASSOCIATED 1 (CCA1) gene disrupts circadian rhythms and suppresses its own expression. Cell **93:** 1207–1217

Xie Q, Wang P, Liu X, Yuan L, Wang L, Zhang C, Li Y, Xing H, Zhi L, Yue Z, et al (2014) LNK1 and LNK2 are transcriptional coactivators in the *Arabidopsis* circadian oscillator. Plant Cell **26:** 2843–2857

Yazdanbakhsh N, Sulpice R, Graf A, Stitt M, Fisahn J (2011) Circadian control of root elongation and C partitioning in Arabidopsis thaliana. Plant Cell Environ **34:** 877–894

Yerushalmi S, Yakir E, Green RM (2011) Circadian clocks and adaptation in Arabidopsis. Mol Ecol **20:** 1155–1165